Continuous Growth of Droplet Size Variance due to Condensation in Turbulent Clouds

Continuous Growth of Droplet Size Variance due to Condensation in Turbulent Clouds

Gaetano Sardina,[1,*] Francesco Picano,[2,3] Luca Brandt,[2] and Rodrigo Caballero[1]
[1]Department of Meteorology and SeRC, Stockholm University, SE-106 91 Stockholm, Sweden
[2]Linné FLOW Centre and SeRC, KTH Mechanics, SE-100 44 Stockholm, Sweden
[3]Department of Industrial Engineering, University of Padova, 35131 Padova, Italy
(Received 15 December 2014; revised manuscript received 21 May 2015; published 29 October 2015)

We use a stochastic model and direct numerical simulation to study the impact of turbulence on cloud droplet growth by condensation. We show that the variance of the droplet size distribution increases in time as $t^{1/2}$, with growth rate proportional to the large-to-small turbulent scale separation and to the turbulence integral scales but independent of the mean turbulent dissipation. Direct numerical simulations confirm this result and produce realistically broad droplet size spectra over time intervals of 20 min, comparable with the time of rain formation.

DOI: 10.1103/PhysRevLett.115.184501 PACS numbers: 47.55.db, 47.27.Gs, 47.55.-t, 92.60.Nv

Many multiscale processes—including nutrient foraging of plankton, gas or dust accretion disks in astrophysics and spray evaporation and combustion in engines [1–4]—involve the interaction between small particles and tracers transported in a turbulent flow. Here we focus on the case of droplet condensation in turbulent warm (i.e. ice-free) clouds. Clouds are a leading source of uncertainty in climate modeling [5] due to the difficulty of accurately parametrizing the macroscale effects of microscale physical processes, such as the effect of droplet size distribution on precipitation rates and cloud albedos.

The role of turbulence in cloud microphysics presents a range of open questions [6–8], particularly as a possible solution for the "bottleneck" problem of rain formation. All cloud droplet populations evolve through a sequence of steps: (1) nucleation or activation of cloud condensation nuclei, (2) droplet growth by condensation, and (3) growth to raindrop size by collision and coalescence. The passage from (2) to (3) presents a bottleneck because collisional growth is only triggered when the droplet population acquires a sufficiently broad size distribution, but condensational growth is inversely proportional to droplet radius which intrinsically tends to narrow the size distribution. Nonetheless, warm clouds are routinely observed to precipitate within $\sim$20 min of formation. Understanding the mechanisms that break the condensational bottleneck is a longstanding and still unresolved problem in atmospheric physics.

Turbulence has often been invoked as a key process in this context since it can enhance collision rates via inertial clustering [9,10] and the so called "sling effect" [11]. Turbulence also induces fluctuations in the supersaturation field that can potentially broaden droplet spectra in the condensational stage [8]. Early studies using analytical models [12,13] and direct numerical simulations (DNS) [14] generally showed too little broadening as compared with observations [15]. Later work attempting to simulate large-scale turbulence in an $O(100\ \mathrm{m})$ cloud [16–18] showed a dramatic broadening of the droplet size spectrum but only with *ad hoc* assumptions about the small-scale supersaturation fluctuations. Lanotte *et al.* [19] modeled both small- and large-scale effects on the droplet size distribution with simulations of a cloud of 70 cm and pointed out the importance of the Taylor Reynolds number, Re_λ, the nondimensional parameter measuring the large- to small-scale separation in homogeneous isotropic turbulence. In particular, they suggested that droplet spectral broadening should scale with $\mathrm{Re}\lambda$.

A question that has not been addressed so far is the long-term fate of the droplet spectrum: does it reach a steady state, or does it continue to evolve? The large range of scales involved makes DNS very computationally demanding, and all existing simulations consider time spans between a few seconds and 2 min, well below the observed rain formation time scale.

Here, we approach this question by first deriving an analytical expression for the standard deviation of the droplet radius squared (droplet surface area) in terms of the thermodynamics and turbulence characteristics, modeling the fluctuations as stochastic processes. We demonstrate that the droplet size distribution increases monotonically with time as $t^{1/2}$. We validate this analytical result by extending previous numerical results with DNS and large eddy simulations (LES) to time scales comparable with those of rain formation, about 20 min. Our results imply that every warm cloud would precipitate if given enough time. The broadening rate is determined by the large scale turbulent motions and by the positive correlation between droplet surface area and local supersaturation.

Our physical model is analogous to that in [19]; a detailed description can be found in the Supplemental Material [20]. We assume homogeneous isotropic turbulence obeying the incompressible Navier-Stokes equations

$$\frac{\partial \mathbf{u}}{\partial t} + \mathbf{u}\cdot\nabla\mathbf{u} = -\frac{\nabla p}{\rho} + \nu\nabla^2\mathbf{u} + \mathbf{f}, \tag{1}$$

where $\mathbf{u}$ is the divergence-free fluid velocity, p the pressure, ρ the air density, $\mathbf{f}$ an external forcing to maintain a statistically stationary state, and ν the kinematic viscosity. This approximation is valid for clouds smaller than $L \approx 100$ m, which allow spatial inhomogeneity and large-scale variations of the thermodynamic parameters to be safely neglected. The supersaturation field s is transported by the fluid according to

$$\frac{\partial s}{\partial t} + \mathbf{u}\cdot\nabla s = \kappa\nabla^2 s + A_1 w - \frac{s}{\tau_s}, \tag{2}$$

a generalization of the Twomey model [27]. The diffusivity of the water vapor in air is denoted by κ, w is the velocity component in the gravity direction, and $A_1 w$ is a source or sink term of supersaturation resulting from the variation in temperature and pressure with height. The supersaturation relaxation time τ_s depends on droplet concentration and dimensions [28], $\tau_s^{-1} = 4\pi\rho_w A_2 A_3 \sum R_i/V$ where R_i are the radii of the droplets in the volume V, ρ_w the water density, and A_1, A_2, and A_3 thermodynamic coefficients [19]. The droplets are assumed to behave as rigid spheres smaller than the Kolmogorov turbulent scale, at low mass fraction to neglect feedback on the flow. The only forces governing the droplet motion are gravity and the Stokes drag (nucleation and activation are not considered):

$$\frac{d\mathbf{v_d}}{dt} = \frac{\mathbf{u}(\mathbf{x_d}, t) - \mathbf{v_d}}{\tau_d} - g\mathbf{e_z}, \qquad \frac{d\mathbf{x_d}}{dt} = \mathbf{v_d} \tag{3}$$

with $\mathbf{x_d}$ and $\mathbf{v_d}$ the droplet position and velocity, $\mathbf{u}(\mathbf{x_d}, t)$ the fluid velocity at droplet position, $\tau_d = 2\rho_w R_i^2/(9\rho\nu)$ the droplet relaxation time, and g the gravitational acceleration. The supersaturation at the droplet position, $s(\mathbf{x_d}, t)$, determines the droplet evolution via

$$\frac{dR_i^2}{dt} = 2A_3 s(\mathbf{x_d}, t). \tag{4}$$

An exact equation for the average of the droplet radius fluctuations is obtained from (4),

$$\frac{d\langle (R_i^{2'})^2\rangle}{dt} = \frac{d\sigma_{R^2}^2}{dt} = 4A_3\langle s' R^{2'}\rangle \tag{5}$$

showing that $\langle (R_i^{2'})^2\rangle$ increases linearly with time only if the correlation $\langle s' R^{2'}\rangle$ reaches a nonzero statistical steady state.

To quantitatively estimate the droplet growth, we adopt a 1D stochastic model for the velocity fluctuations w_i and the supersaturation field s_i' of the ith droplet. Such an approach implicitly assumes that the small-scale turbulent motions have a negligible influence on the macroscopic observables. This assumption is motivated by previous results revealing the broadening of the droplet size distribution with Re_λ [19] and fully justified *a posteriori* by the numerical simulations presented below.

Homogeneous isotropic turbulence and supersaturation are modeled with two Langevin equations [29]:

$$w_i'(t+dt) = w_i'(t) - \frac{w_i'(t)}{T_0}dt + v_{\mathrm{rms}}\sqrt{2\frac{dt}{T_0}}\xi_i(t), \tag{6}$$

where v_{rms} is the root mean square of the turbulent velocity fluctuations, $\xi(t)$ is a zeromean Gaussian white noise, nondimensionalized in order to be δ correlated in time and T_0 the turbulence integral time scale, and

$$\begin{aligned} s_i'(t+dt) = s_i'(t) &- \frac{s_i'}{T_0}dt + A_1 w_i' dt - \frac{s_i'}{\langle\tau_s\rangle}dt \\ &+ \sqrt{(1-C_{ws}^2)\langle s'^2\rangle\frac{2dt}{T_0}}\eta_i(t) \\ &+ C_{ws}\sqrt{\langle s'^2\rangle\frac{2dt}{T_0}}\xi_i(t) \end{aligned} \tag{7}$$

for the supersaturation with forcing from the velocity field. Here $C_{ws} = \langle w's'\rangle/(v_{\mathrm{rms}}\sqrt{\langle s'^2\rangle})$ is the normalized velocity-supersaturation correlation, and $\langle\tau_s\rangle$ is the supersaturation relaxation time based on the mean droplet radius and $\eta(t)$ zero-mean Gaussian white noise, δ correlated in time. Equation (7) represents a stochastic version of the Twomey model. The mean updraft is zero as the mean supersaturation (the mean droplet radius does not change); entrainment effects [30], collisions, and inhomogeneities are also not considered to analyze the conservative case when the droplet spectral broadening is only induced by supersaturation fluctuations.

From (4), (6), and (7), assuming $\langle\tau_s\rangle \ll T_0$ as in real clouds, the fluctuation correlations become

$$\frac{d\langle s' R^{2'}\rangle}{dt} = A_1\langle w' R^{2'}\rangle + 2A_3\langle s'^2\rangle - \frac{\langle s' R^{2'}\rangle}{\langle\tau_s\rangle}, \tag{8}$$

$$\frac{d\langle w' R^{2'}\rangle}{dt} = 2A_3\langle w's'\rangle - \frac{\langle w' R^{2'}\rangle}{T_0}, \tag{9}$$

$$\frac{d\langle s'^2\rangle}{dt} = 2A_1\langle w's'\rangle - 2\frac{\langle s'^2\rangle}{\langle\tau_s\rangle}, \tag{10}$$

$$\frac{d\langle w's'\rangle}{dt} = A_1 v_{\mathrm{rms}}^2 - \frac{\langle w's'\rangle}{\langle\tau_s\rangle}. \tag{11}$$

Assuming statistically quasisteady state conditions ($d\langle\rangle/dt = 0$) we find that $\langle s'^2\rangle_{qs} = A_1^2 v_{\mathrm{rms}}^2\langle\tau_s\rangle^2$ and

$$\langle s' R^{2'} \rangle_{qs} = 2A_3 A_1^2 v_{\rm rms}^2 \langle \tau_s \rangle^2 T_0 = 2A_3 \langle s'^2 \rangle_{qs} T_0 \qquad (12)$$

which give, using (5),

$$\sigma_{R^2} = \sqrt{8} A_3 A_1 v_{\rm rms} \langle \tau_s \rangle (T_0 t)^{1/2} = \sqrt{8 \langle s'^2 \rangle_{qs}} A_3 (T_0 t)^{1/2}. \qquad (13)$$

The model shows that the variance of the droplet distribution increases monotonically in a turbulent flow even though the supersaturation fluctuations reach a statistical steady state s_{qs}. The correlation $\langle s' R^{2'} \rangle_{qs}$, which is directly responsible for the radius growth rate, is proportional to the level of fluctuations of the supersaturation field and to the integral scale of the turbulence; see (12). Expression (13) can be formulated in terms of Kolmogorov scales since $v_{\rm rms} \simeq {\rm Re}_\lambda^{1/2} v_\eta$ and $T_0 \simeq 0.06 {\rm Re}_\lambda \tau_\eta$ [29]:

$$\sigma_{R^2} \simeq 0.7 A_3 A_1 \nu^{1/2} \langle \tau_s \rangle {\rm Re}_\lambda t^{1/2}. \qquad (14)$$

Note that for $t = T_0$ (short compared with rain formation time) the lower limit proposed in [19] is recovered, $\sigma_{R^2} \simeq {\rm Re}_\lambda^{3/2}$. From (14) we note that σ_{R^2} at a fixed time depends only on the scale separation represented by ${\rm Re}_\lambda$ and not on the value of the mean dissipation inside the clouds. This implies that clouds with different dissipation rate and same Reynolds number have an identical behavior in terms of droplet growth by condensation. The droplet or turbulence condensation dynamics does not depend on the turbulent small scales: the correlation between the supersaturation field and the droplet surface area, governing the distribution broadening, is determined by the large flow scales. This result is in contrast with the belief that the variance of the droplet distribution should not grow indefinitely as turbulence tends to decorrelate the particle size from the local saturation field [8].

To test our predictions, we run simulations by gradually increasing the size of the computational clouds from a few centimeters to 100 m. The governing equations (1)–(4) are solved with a classical pseudospectral code for the fluid phase coupled with a Lagrangian algorithm for the droplets [31]. All cases share the same turbulent kinetic energy dissipation $\varepsilon = 10^{-3}$ m^2 s^{-3}, a value typically measured in stratocumuli. This corresponds to the same small-scale dynamics, with Kolmogorov scale $\eta = (\nu^3/\varepsilon)^{1/4} \approx 1$ mm, Kolmogorov time $\tau_\eta = (\nu/\varepsilon)^{1/2} \approx 0.1$ s, and velocity $v_\eta = \eta/\tau_\eta \approx 1$ cm/s. We examine droplets with two different initial radii, 13 μm and 5 μm, denoted as case 1 and 2, with supersaturation relaxation time $\tau_s = 2.5$ and 7 s, and same concentration (130 droplets per cm^3). The reference temperature and pressure are $\theta_0 = 283$ K and $P = 10^5$ Pa, with $A_1 = 5 \times 10^{-4}$ m^{-1}, $A_2 = 350$ m^3/kg, and $A_3 = 50$ μm^2/s. The simulation parameters are reported in Table I. Note that simulation DNS E1, carrying order 10^9 droplets, is to the best of our knowledge the largest direct numerical simulation of a warm cloud ever performed.

TABLE I. Parameters of the simulations. The resolution N, the cloud size $L_{\rm box}$, the root mean square of the turbulent velocity fluctuations $v_{\rm rms}$, and $T_L = L_{\rm box}/v_{\rm rms}$ an approximation of the large turbulent scales. T_0 indicates the integral time $T_0 = (\pi/2v_{\rm rms}^3) \int [E(k)/k] dk$ with k the wave number and $E(k)$ the turbulent kinetic energy spectra [29]. The total number of droplets is indicated by N_d.

Label	N^3	$L_{\rm box}$ [m]	$v_{\rm rms}$ [m/s]	T_L [s]	T_0 [s]	${\rm Re}_\lambda$	N_d
DNS $A1/2$	64^3	0.08	0.035	2.3	0.64	45	6×10^4
DNS $B1/2$	128^3	0.2	0.05	4	0.95	95	9.8×10^5
DNS $C1/2$	256^3	0.4	0.066	6	1.5	150	9×10^6
DNS D1	1024^3	1.5	0.11	14	3	390	4.4×10^8
DNS E1	2048^3	3	0.12	30	4	600	$3. \times 10^9$
LES F1	512^3	100	0.7	142	33	5000	1.3×10^{14}

The time evolution of $\sigma_{R^2} = \sqrt{\langle (R^{2'})^2 \rangle}$ is shown in Fig. 1 for all cases investigated. The data confirm the predictions from (13), i.e. that $\sigma_{R^2} \propto t^{1/2}$.

The correlation $\langle s' R^{2'} \rangle$ is displayed in the inset of Fig. 1 (thin solid line). In all cases, $\langle s' R^{2'} \rangle$ reaches a statistical steady state, fluctuating around the value determining the growth of σ_{R^2}. The turbulence creates a positive correlation between supersaturation and droplet surface area fluctuations that increases as the turbulent scale separation—i.e. the cloud size—increases. The agreement between the model and the numerical data is remarkable for the largest domain sizes where scale separation is significant and

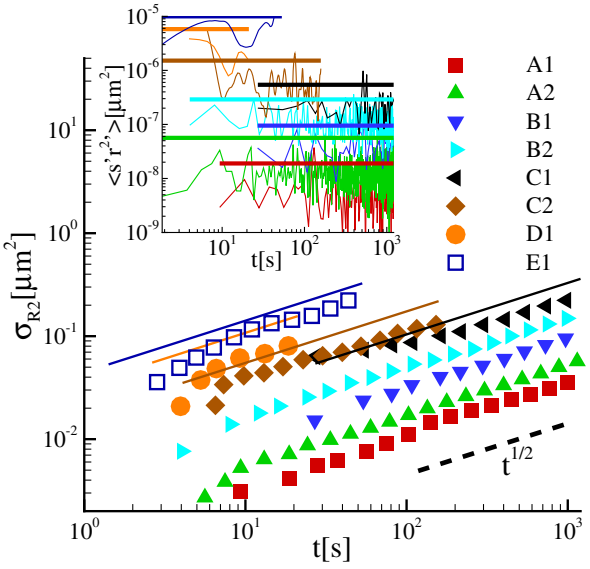

FIG. 1 (color online). Root mean square of the square droplet radius fluctuations σ_{R^2} versus time from simulations (symbols) and the prediction of the stochastic model (13) (lines). Inset: correlation $\langle s' R^{2'} \rangle$ from simulations (thin lines) and from Eq. (12) (thick lines).

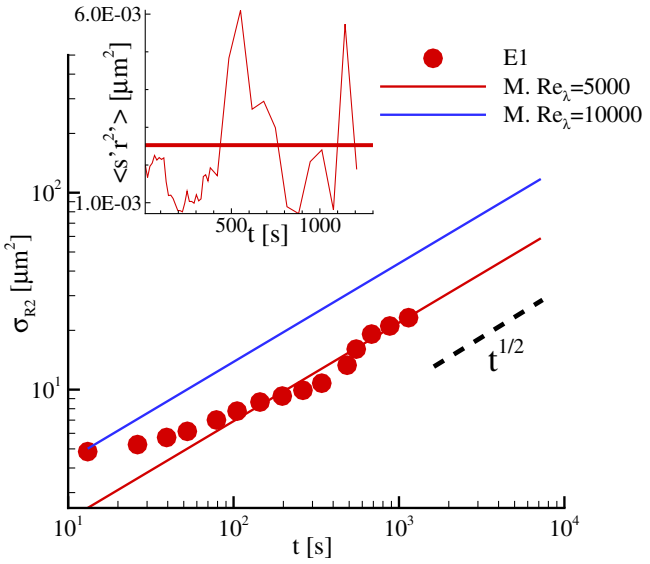

FIG. 2 (color online). Root main square of the square droplet radius fluctuations σ_{R^2} versus time for the LES simulations (symbols) and the model (13) (lines). Inset: correlation $\langle s'R^{2'}\rangle$ from the LES (thin line) and the model (12) [denoted by "M." in the legend (thick lines)].

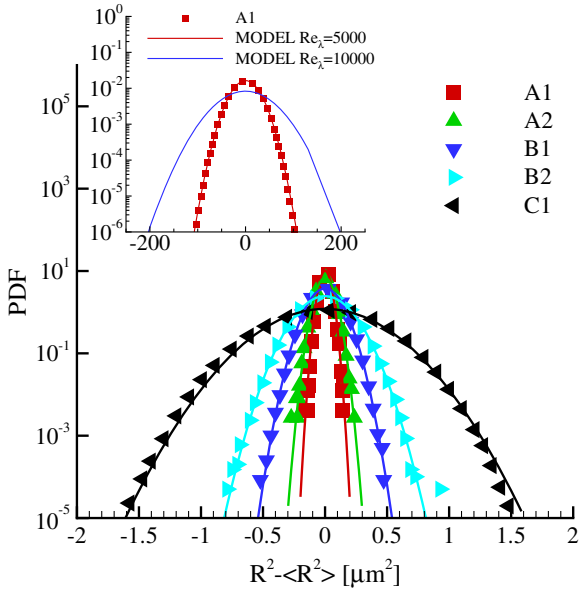

FIG. 3 (color online). Probability density functions (PDFs) of the square radius fluctuations after a simulation time corresponding to about 20 min. (symbols). The lines represent Gaussian distributions with the same variance. The inset reports data from the LES of a large cloud.

viscous effects can be neglected. For small Re_λ, viscous effects are important and the stochastic inviscid model overestimates the correct behavior. For a detailed comparison between DNS and stochastic model, see the Supplemental Material [20].

To test the model for a larger cloud size, we perform a large eddy simulation (LES F1) of a cloud of about 100 m. LES can be seen as a good model for our problem since it fully resolves the larger flow scale, those relevant to droplet condensation or evaporation, as shown above. For numerical details see the Supplemental Material [20]. The Taylor Reynolds number is 5000. The time evolutions of σ_{R^2} and of $\langle s'R^{2'}\rangle$ are depicted in Fig. 2 together with the analytical predictions from (12) and (13). The agreement between the two fully validates our model.

To motivate the use of the variance $\sigma^2_{R^2}$ to define the droplet size distribution, we show in Fig. 3 that its probability distribution is Gaussian, in agreement with measurements in real stratocumuli [32]. The data in the figure refer to the final simulation time (about 20 min) and are compared to Gaussian distributions of equal variance; note that error bars are about the same size as the plotting symbols and not visible in the plot. The size distribution from the LES of the large cloud (see inset) reveals that the Gaussian can be fitted just using the value of σ_{R^2} from the stochastic model also at this higher Reynolds number.

In summary, we have derived an analytical expression for the role of turbulence on the dynamics of droplet condensation and validated it against large-scale numerical simulations. We show that the standard deviation of the square droplet radius fluctuations, σ_{R^2}, increases in time as $t^{1/2}$; the growth rate depends linearly on the turbulent scale separation parametrized by Re_λ. As shown in Fig. 2, for a cloud with $\mathrm{Re}_\lambda = 10000$—a typical value estimated in cumuli with integral scale of 100 m [8]—our expression predicts that σ_{R^2} reaches values in line with observations in real clouds (see [15], their Fig. 4) on time scales of less than 20 min.

The stochastic approach proposed here may be generalized to consider additional physics and adapted to different microscale phenomena in turbulent environments; this may also require a numerical solution of the governing Langevin equations, something still order of magnitudes cheaper than a fully-resolved DNS. Indeed our analytical relation predicts numerical results requiring 10^{17} degrees of freedom. From a practical viewpoint, this indicates the promising potential of modeling approaches based on PDFs.

Our results represent a lower limit for the impact of turbulence on warm rain formation since real clouds typically exceed 100 m in scale and are in general nonhomogeneous, featuring a fluctuating temperature field and vigorous entrainment of relatively dry air from outside the cloud leading to enhanced supersaturation fluctuations within the cloud. These additional effects would lead to even larger values of σ_{R^2}, more than sufficient to explain the spectral broadening observed in real clouds.

This work was supported by the Swedish e-Science Research Centre SeRC, and by the European Research Council Grant No. ERC-2013-CoG-616186, TRITOS. Computer time provided by SNIC (Swedish National Infrastructure for Computing) is gratefully acknowledged.

*gaetano.sardina@misu.su.se

[1] J. R. Taylor and R. Stocker, Science **338**, 675 (2012).
[2] A. Johansen, J. S. Oishi, M.-M. Mac Low, H. Klahr, T. Henning, and A. Youdin, Nature (London) **448**, 1022 (2007).
[3] P. Jenny, D. Roekaerts, and N. Beishuizen, Prog. Energy Combust. Sci. **38**, 846 (2012).
[4] J. Bec, H. Homann, and G. Krstulovic, Phys. Rev. Lett. **112**, 234503 (2014).
[5] H. Shiogama and T. Ogura, Nature (London) **505**, 34 (2014).
[6] R. A. Shaw, Annu. Rev. Fluid Mech. **35**, 183 (2003).
[7] E. Bodenschatz, S. P. Malinowski, R. A. Shaw, and F. Stratmann, Science **327**, 970 (2010).
[8] W. W. Grabowski and L.-P. Wang, Annu. Rev. Fluid Mech. **45**, 293 (2013).
[9] S. Sundaram and L. R. Collins, J. Fluid Mech. **335**, 75 (1997).
[10] J. Bec, H. Homann, and S. S. Ray, Phys. Rev. Lett. **112**, 184501 (2014).
[11] G. Falkovich, A. Fouxon, and M. Stepanov, Nature (London) **419**, 151 (2002).
[12] W. A. Cooper, J. Atmos. Sci. **46**, 1301 (1989).
[13] M. Kulmala, Ü. Rannik, E. L. Zapadinsky, and C. F. Clement, J. Aerosol Sci. **28**, 1395 (1997).
[14] P. Vaillancourt, M. Yau, and W. Grabowski, J. Atmos. Sci. **58**, 1945 (2001).
[15] J.-L. Brenguier and L. Chaumat, J. Atmos. Sci. **58**, 628 (2001).
[16] A. Celani, A. Mazzino, A. Seminara, and M. Tizzi, J. Turbul. **8**, N17 (2007).
[17] A. Celani, G. Falkovich, A. Mazzino, and A. Seminara, Europhys. Lett. **70**, 775 (2005).
[18] R. Paoli and K. Shariff, J. Atmos. Sci. **66**, 723 (2009).
[19] A. S. Lanotte, A. Seminara, and F. Toschi, J. Atmos. Sci. **66**, 1685 (2009).
[20] See Supplemental Material at http://link.aps.org/supplemental/10.1103/PhysRevLett.115.184501, which includes Refs. [21–26], for details on the physical models, further information on the numerical scheme, and additional results.
[21] H. Siebert, K. Lehmann, and M. Wendisch, J. Atmos. Sci. **63**, 1451 (2006).
[22] B. Kumar, J. Schumacher, and R. A. Shaw, Theor. Comput. Fluid Dyn. **27**, 361 (2013).
[23] P. A. Vaillancourt and M. K. Yau, Bull. Am. Meteorol. Soc. **81**, 285 (2000).
[24] R. Rogallo, Numerical experiments in homogeneous turbulence, NASA Technical Report No. 81835, 1981.
[25] V. Eswaran and S. Pope, Comput. Fluids **16**, 257 (1988).
[26] J. Smagorinsky, Mon. Weather Rev. **91**, 99 (1963).
[27] S. Twomey, Pure Appl. Geophys. **43**, 243 (1959).
[28] H. Pruppacher and J. Klett, *Microphysics of Clouds and Precipitation* (Kluwer Academic, Dordrecht, 1997).
[29] S. B. Pope, *Turbulent Flows* (Cambridge University Press, Cambridge, England, 2000).
[30] B. Kumar, J. Schumacher, and R. A. Shaw, J. Atmos. Sci. **71**, 2564 (2014).
[31] C. Zhan, G. Sardina, E. Lushi, and L. Brandt, J. Fluid Mech. **739**, 22 (2014).
[32] F. Ditas, R. Shaw, H. Siebert, M. Simmel, B. Wehner, and A. Wiedensohler, Atmos. Chem. Phys. **12**, 2459 (2012).